Pressure Drop for Cocurrent Downflow of Gas-Solids Suspensions

Pressure drop for a gas-solids suspension flowing concurrently downward in a 13-mm inside-diameter tube was investigated using 329-micron spherical glass beads in air. The gas Reynolds number varied from 0 to 30,000 with solids-loading ratios of up to 20 at a gas Reynolds number of 10,000. The frictional pressure drop for downflow was found to be a weaker function of the solids-loading ratio than the upflow case using data reported in the literature. Empirical correlation of the two-phase friction factor, in terms of the gas Reynolds number and a dimensionless parameter, $C_D E_p D/[(1 - E_p)d_p]$, showed that at high solids loadings, particles tend to stabilize the suspension flow. The dimensionless parameter seems to be applicable to a universal pressure drop correlation for solids-fluid systems, but requires further investigation.

J. M. KIM and J. D. SEADER

University of Utah
Dept. of Chemical Engineering
Salt Lake City, UT 84112

SCOPE

Gas-solids suspension flows are encountered in many industrial processes. A few examples are: pneumatic conveying and drying in gas-solid handling systems, catalytic cracking and reforming processes, nuclear reactor cooling systems, and the combustion of pulverized coal. Recent applications of various gas-solid reactors to coal-conversion processes have prompted a new interest toward the understanding of flow and heat transfer characteristics of gas-solids suspension. In a short-residence-time transport reactor, the coal particles and hydrogen flow cocurrently downward through a tubular reactor, while being heated through the tube wall (Ladelfa et al., 1977; Wood and Wiser, 1976). Under a short-residence-time condition, the overall reaction rate would be greatly affected by transport phenomena such as heat transfer and flow characteristics of the gas-solid suspension in the reactor.

While numerous investigations of the flow characteristics of gas-solids suspensions have been conducted in the past, most have been concerned with vertical-upflow or horizontal-flow systems. The vertical-downflow system has been largely neglected. Recently, limited data on pressure drop for the vertical-downflow case were reported in a paper by Shimizu et al. (1978). However, they studied pressure drop for the vertical-downflow system as a peripheral problem to their main investigation of the vertical-upflow case; and they conceded that their downflow data were not complete and trustworthy.

The primary objective of this study was to conduct an investigation of the flow characteristics of gas-solids suspensions in a cocurrent-downflow system by obtaining pressure-drop data using well-defined, closely sized glass beads in air. The next objective was to develop correlations for the pressure-drop data, and to clarify the difference between the upflow and downflow cases by comparing the present data with those reported in the literature for the upflow system.

CONCLUSIONS AND SIGNIFICANCE

Pressure drop profiles along the tube revealed that the hydraulic entry length is greatly extended by the addition of particles (up to 300 tube diameters at the solids flow rate of 182 kg/h) and is more dependent on the solids flow rate than on the gas Reynolds number. In downflow, a negative total pressure drop can occur; however, if the static head effect is accounted for by adding the weight of particles, the resulting frictional pressure drop becomes positive and is found to be a weak function of solids-loading ratio. Comparison of the present data with the upflow results in the literature shows that, for solids-loading ratios greater than about three, the frictional pressure drop in downflow becomes smaller than in upflow.

The frictional pressure drop is correlated in terms of the two-phase friction factor, which is a function of gas Reynolds number and a dimensionless parameter, $C_D E_p D/[(1 - E_p)d_p]$, derived from a similarity analysis of the governing equations of suspension flow. The correlation indicates that the presence of particles has a stabilizing effect on suspension flow in the transition region. It is also shown that the pressure drop through a packed bed as given by Ergun's equation can be recorrelated in terms of the new parameter. Comparison of the correlations for dilute-phase transport and the packed bed indicates that the parameter, $C_D E_p D/[(1 - E_p)d_p]$, may find applicability in correlating the frictional pressure drop for general gas-solids systems; further study is necessary to confirm this suggestion.

LITERATURE REVIEW

The study of gas-solids suspension flow has received considerable attention in the past because of its importance in various chemical engineering processes. Literature on this subject is abundant (Boothroyd, 1971; Soo, 1967). However, progress toward understanding has been slow, and much experimental data reported in the literature are in conflict. Several pressure-drop correlations proposed for vertical-upflow systems cover a very limited range of variables, and they cannot be safely extrapolated outside the range of the experimental data.

Correspondence concerning this paper should be addressed to J. D. Seader. J. M. Kim is presently with C. F. Braun & Co., Alhambra, CA.

0001-1541-83-6881-0353-$2.00.

Early investigations of pressure drop for gas-solids suspension flow, mainly concerned with pneumatic transport of various solid particles through vertical or horizontal pipes, were carried out by Gasterstaedt (1924), Vogt and White (1948), and Farber (1949). These works generally confirmed a linear relationship between the specific pressure drop, which was defined as the ratio of the total pressure drop of the suspension to that for gas alone at the same gas flow rate, and the solids-loading ratio. Hariu and Molstad (1949) separated the total frictional pressure drop into two components:

$$\Delta P_f = \Delta P_{fg} + \Delta P_{fp} = \Delta P_t - \Delta P_{\rho p} \tag{1}$$

They assumed that the frictional pressure drop due to the gas, ΔP_{fg}, was the same as that for the flow of gas alone, effectively including the excess pressure drop due to addition of particles in the term ΔP_{fp}. A correlation of ΔP_{fp} was then proposed by defining the solids friction factor in terms of the dispersed particle density and particle velocity:

$$f_p = \frac{\Delta P_{fp} D}{2L\rho_{dp} U_p{}^2} \tag{2}$$

The concept of a solids friction factor has been extended by many other investigators, including Rose and Barnacle (1957), Richardson and McLeman (1970), Jones et al. (1967), Capes and Nakamura (1973), Konno and Saito (1969), Leung and Wiles (1976), and Yang (1978).

Contrary to the solids-friction factor approach, Mehta et al. (1957) proposed a correlation that did not assume that the pressure drop due to gas was unaffected by the solid particles. They defined a mixture friction factor, f_m, as

$$\Delta P_f = \frac{f_m L \rho_g U_g^2}{2g_c D}\left[1 + \left(\frac{\rho_{dp} U_p^2}{\rho_{dp} U_g^2}\right)^a\right] \tag{3}$$

where a was a constant chosen by the authors as 0.3 for 36-micron glass spheres and 1.0 for 97-micron glass spheres. The mixture friction factor was found to be a function of particle size, solids flow rate, and gas Reynolds number. Julian and Dukler (1965) suggested that the solids made their influence felt primarily by modifying the local turbulence in the gas phase, increasing the turbulence fluctuations, mixing length, eddy viscosity, and thus the frictional pressure drop. They modified the Gill and Sher (1961) eddy viscosity equation for single-phase flow through a tube by redefining the Von Karman constant as a function of the solids-loading ratio.

Rose and Duckworth (1969) developed general, but complicated, graphical correlations for the prediction of pressure drop by applying dimensional analysis to the individual pressure-drop components of the equation

$$\Delta P_t = \Delta P_{ag} + \Delta P_{ap} + \Delta P_{fg} + \Delta P_{fp} + \Delta P_{\rho g} + \Delta P_{\rho p} \tag{4}$$

Khan and Pei (1973) conducted a comparative study of the existing correlations for the pressure drop in dilute-phase vertical transport and presented a correlating equation of the ratio of the friction pressure drop for the suspension to that for gas alone.

Recently, Shimizu et al. (1978) reported limited experimental data on vertical downflow along with their main study of pressure drop in vertical upward flow of copper particles. The gas Reynolds number varied up to 50,000 with solids-loading ratios up to 5. Comparison of the pressure gradients along the tube for the upflow and downflow cases showed that the acceleration length in the downflow case was longer than that for the upflow case. Unfortunately, the test section for the vertical downflow experiment, 3.81 m in length, was found to be too short to realize a fully developed flow condition even at the lowest section of the tube. Hence, they reported that their data for downflow, which showed very high pressure drops at high Reynolds numbers, were not trustworthy.

Many investigators have studied the flow pattern of suspension flows, such as: particle and gas velocities by Doig and Roper (1967), Reddy and Pei (1969), and Kramer (1970); particle concentration distribution by Soo and Regalbuto (1960), Kramer (1970), and Gel'perin et al. (1976). These investigations generally revealed certain aspects of flow characteristics, but as yet the effect of particles on the gas flow field is not fully understood.

Theoretical studies of gas-solids suspension flows have been approached in two ways. First, the results of the dynamics of a single particle in a turbulent-flow field was extended to multiparticle systems (Soo, 1962; Friedlander, 1957; Peskin, 1959). However, because of difficulties associated with the proper description of particle collisions, flow field changes between particles, and wall effects, most recent work has adopted a second approach that involves application of continuum mechanics to suspension flow with modifications (Van Deemter, 1961; Hinze, 1962; Soo, 1967; Kramer and Depew, 1972). Although important for the understanding of fundamental mechanisms involved, rigorous theoretical treatments have produced solutions only for very dilute suspensions.

SIMILARITY ANALYSIS

Conservation equations for a suspension flow in the axial direction, assuming that radial and tangential components are negligible, can be written as

Continuity Equations

$$\text{gas:}\quad \frac{\partial}{\partial t}[(1-E_p)\rho_g] + \frac{\partial}{\partial x}[(1-E_p)\rho_g U_g] = 0 \tag{5}$$

$$\text{particles:}\quad \frac{\partial}{\partial t}[E_p\rho_p] + \frac{\partial}{\partial x}[E_p\rho_p U_p] = 0 \tag{6}$$

$$\text{mixture:}\quad \frac{\partial}{\partial t}[(1-E_p)\rho_g + E_p\rho_p] + \frac{\partial}{\partial x}[(1-E_p)\rho_g U_g + E_p\rho_p U_p] = 0 \tag{7}$$

Momentum Equations

$$\text{gas:}\quad \frac{\partial}{\partial t}[(1-E_p)\rho_g U_g] + \frac{\partial}{\partial x}[(1-E_p)\rho_g U_g^2] = -\frac{\partial}{\partial x}[(1-E_p)P] + \frac{\mu_{gm}}{r}\frac{\partial}{\partial r}\left(r\frac{\partial U_g}{\partial r}\right) + (1-E_p)\rho_g g - \frac{3E_p C_D \rho_g}{4d_p}(U_g - U_p)^2 \tag{8}$$

$$\text{particles:}\quad \frac{\partial}{\partial t}[E_p\rho_p U_p] + \frac{\partial}{\partial x}[E_p\rho_p U_p^2] = -\frac{\partial}{\partial x}[E_p P] + \frac{\mu_{pm}}{r}\frac{\partial}{\partial r}\left(r\frac{\partial U_p}{\partial r}\right) + E_p\rho_p g + \frac{3E_p C_D \rho_g}{4d_p}(U_g - U_p)^2 \tag{9}$$

$$\text{mixture:}\quad \frac{\partial}{\partial t}[(1-E_p)\rho_g U_g + E_p\rho_p U_p] = -\frac{\partial}{\partial x}[(1-E_p)\rho_g U_g^2 + E_p\rho_p U_p^2] - \frac{\partial p}{\partial x} + \frac{\mu_{gm}}{r}\frac{\partial}{r}\left(r\frac{\partial U_g}{\partial r}\right) + \frac{\mu_{pm}}{r}\frac{\partial}{\partial r}\left(r\frac{\partial U_p}{\partial r}\right) + [(1-E_p)\rho_g + E_p\rho_p]g \tag{10}$$

The above equations are exact for laminar flow. In case of turbulent flow, we regard the variables as time-averaged values and presume, from an analogy with single-phase flow, that the same correlating parameters as given later hold for both laminar and turbulent flow.

In problems where a complete solution of differential equations and boundary conditions is not possible or feasible, the minimal set of dimensionless groups as well as the relationships among these groups may be found using similarity analysis as suggested by

Hellums and Churchill (1961) and Churchill (1974). As shown by Kim (1979), when their procedures are applied to the steady-state forms of Eqs. 5, 7, 8 and 10 the following relations can be written for the two-phase friction factor:

$$f_{tp} = \psi_1 \left[\frac{DU_{sg}\rho_g}{\mu_g} , \frac{\rho_p}{\rho_g} , \frac{W_p}{W_g} , \frac{C_D E_p D}{(1 - E_p)d_p} \right] \tag{11}$$

where f_{tp} is defined as

$$f_{tp} = \frac{\Delta P_f D}{2\rho_g U_{sg}^2 L} \tag{12}$$

It should be noted that the two-phase friction factor is defined here in terms of the frictional pressure drop, which includes contributions due to both gas and particles. This definition is preferred over the solids-friction factor because the nature of turbulence in the gas phase is expected to change progressively as more particles are added to the flow so that the contributions of either phase cannot be evaluated separately.

In a strict sense, complete elimination of any explicit parameter in Eq. 11 is not possible. However, further simplification of the functional relationship may be made by noting that the particle holdup appearing in the term $C_D E_p D/[(1 - E_p)d_p]$ is related to the loading ratio, as shown in Figure 6 in a later section, and to the density ratio. Accordingly, Eq. 11 may be simplified to the form

$$f_{tp} = \psi_2 \left[\frac{DU_{sg}\rho_g}{\mu_g} , \frac{C_D E_p D}{(1 - E_p)d_p} \right] \tag{13}$$

The first group on the righthand side of Eq. 13 is the gas Reynolds number based on the superficial gas velocity, and the second dimensionless group is an indication of the amount of solids present in the suspension. This parameter will be designated as α in subsequent discussions.

The drag coefficient of particles in a suspension, C_D, is given by Wen and Yu (1966) in terms of the single-particle drag coefficient and the particle concentration as

$$(C_D)_{U_{sg}} = (C_{D,s})_{U_{sg}}(1 - E_p)^{-4.7} \tag{14}$$

where $(C_D)_{U_{sg}}$ and $(C_{D,s})_{U_{sg}}$ are the drag coefficient in a suspension and in an infinite fluid based on the same superficial velocity. Based on the actual interstitial velocity, Eq. 14 becomes

$$C_D = C_{D,s}(1 - E_P)^{-(2.7+n)} \tag{15}$$

where

$$n \simeq 0.64 \quad \text{for } N_{Re,p} < 500,$$
$$n \simeq 300/N_{Re,p} \quad \text{for } N_{Re,p} > 500.$$

As shown later, experimental pressure-drop data were correlated using the parameters in Eq. 13, which also includes single-phase flow as the lower limiting case where α goes to zero. General applicability of Eq. 13 over the full range of particle holdup was also studied by recorrelating the pressure drop in a packed bed in terms of the parameters in the equation and by comparing the results with those for dilute-phase transport. The pressure drop through a packed bed was obtained from Ergun's equation (1952):

$$\frac{\Delta P_f}{L} = \frac{E_p^2}{(1 - E_p)^3} \frac{\mu_g U_{sg}}{d_p^2} + 1.75 \frac{E_p}{(1 - E_p)^3} \frac{\rho_g U_{sg}^2}{d_p} \tag{16}$$

EXPERIMENTAL

Apparatus and Procedure

The overall experimental apparatus consisted of three subsystems, gas-flow system, particles feed and return system, and pressure drop and holdup test section. Figure 1 shows a schematic flow diagram of the apparatus. The air drawn through pressure regulators, a filter dryer unit, and rotameters, was introduced to a mixing chamber where particles were added. The mixing chamber had two inside air-distribution guides, which directed the air downward to prevent violent mxing with the particles on entering the tube. The particles were fed by a vibratory feeder with a tubular trough

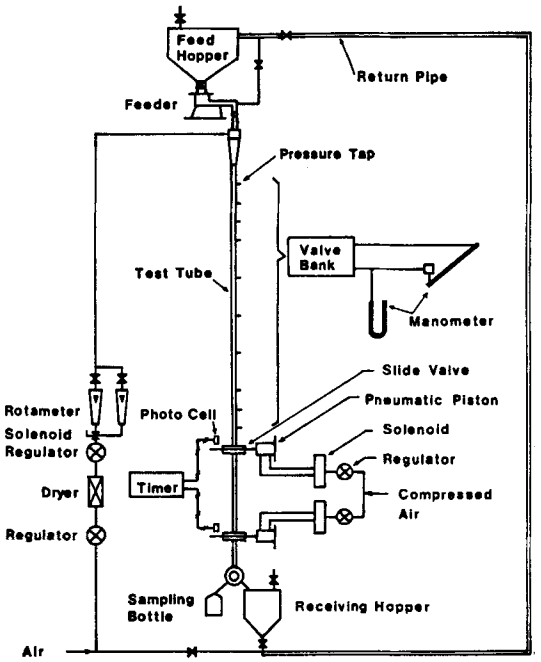

Figure 1. Schematic diagram of overall apparatus.

operated by a remote controller. After leaving the mixing chamber, the gas-solids suspension flowed through the approach section, the holdup section, and into the receiving hopper, where the air was exhausted into the room through a screen filter. A three-way valve at the end of the tube permitted sampling of the stream for solids flow rate measurement. The particles collected in the receiving hopper were transported to the feed hopper through a return pipe.

The 0.91-m-long holdup test section and the 6.71-m approach section, along which the pressure drops were measured, were made of type 304 stainless-steel seamless tubing with a 13-mm inside diameter and 3.05-mm wall thickness. Pressure tap holes, 1.6 mm in diameter, were drilled in the approach section at 10 axial locations, as shown in Figure 1. The first four taps and the last three taps from the top were more closely spaced (0.518 m apart) than the taps in between, which were spaced 1.035 m apart. The inside edges of the pressure tap holes were carefuly deburred and sanded with fine sand papers to give smooth surfaces.

Pressure drops were measured with an inclined manometer which had a maximum range of 20.3 cm with 0.25-mm graduations. A glass U-tube manometer measured absolute pressures. The pressure taps were connected to the manometers through a bank of three-way ball valves in such a way that the pressure drop between any desired set of taps could be read on the inclined manometer, the absolute pressure of one tap being read on the U-tube manometer. Particle-trapping cylinders, which were installed between the pressure taps and the valve banks, protected the valves from being damaged by entrapped particles in the pressure lines.

The holdup test section had slide valves at both ends. Each valve, fabricated from a 6.35-cm-diameter, stainless-steel bar, consisted of two separable valve body pieces and a slider between the grove in the valve body. Teflon sleeves set into the groove compressed against the slider to provide a tight seal with the least amount of friction between the moving slider. The compression pressure could be adjusted by two screws in the valve body. A narrow reflecting slit of 0.7-mm width near the end of the slider was used for measuring the closing time of the individual valve and the starting time difference between the top and bottom valves by a dual-mode digital timer with photocells as sensors. The slide valves were operated by double-acting air pistons to which compressed air lines were connected through four-way pneumatic valves with electrical solenoid-pilot actuators. Pressure regulators before the pneumatic valves kept the air pressure at about 0.88 MPa. A common electrical switch was used for the solenoid-pilot actuators to close the slide valves simultaneously. Both valves were closed in 10 ms with an average starting time difference of about 0.9 ms. Errors in holdup measurements caused by the starting time differences were found to be negligible (Kim, 1979).

The particles used were Ballotini soda lime glass beads with an average diameter, based on length, of 329 micron. This diameter was the average of a sample of 130 glass beads, ranging in size from minus 45/plus 50 mesh (U.S. Series), as measured under a microscope fitted with a micrometer eyepiece. The density of the particles was 2.48 g/cm^3.

Experiments were carried out at various gas Reynolds numbers up to

30,000. The maximum solids flow rate was 182 kg/h, which corresponded to a loading ratio of nearly 20 at a gas Reynolds number of 10,000. All experiments were conducted under room temperature conditions. The operation of the apparatus was checked by running experiments with air alone, for which complete pressure-drop profiles were measured to locate and correct any defective parts in the pressure taps, particle-trapping cylinders, and pressure-line valves.

Analysis of Data

Integration of steady-state forms of Eqs. 5 and 6 yields the following macroscopic continuity equations, which relate superficial and actual velocities in suspension flow:

$$\rho_g(1 - E_p)U_g = G_g = \rho_g U_{sg} \tag{17}$$

$$\rho_p E_p U_p = G_p = \rho_p U_{sg} \tag{18}$$

hence

$$U_g = \frac{U_{sg}}{1 - E_p}, \quad U_p = \frac{U_{sp}}{E_p} \tag{19}$$

and

$$V_s = U_g - U_p = \frac{U_{sg}}{1 - E_p} - \frac{U_{sp}}{E_p} \tag{20}$$

Equations 19 and 20 permit calculations of the particle velocity and slip velocity from the particle holdup data, which were obtained from the particle weight trapped between the slide valves.

The total pressure drop in a suspension flow is given by

$$\Delta P_t = [\Delta P_{ag} + \Delta P_{ap}] - [\Delta P_{pg} + \Delta P_{\rho p}] + \Delta P_f \tag{21}$$

where the five terms on the righthand side of the equation are the pressure drop due to gas acceleration, particle acceleration, gas static head, particle static head, and friction. The sign before $[\Delta P_{\rho g} + \Delta P_{\rho p}]$ becomes positive in case of upward flow. Neglecting the acceleration pressure drop in the fully developed region, the friction pressure drop can be calculated from

$$\Delta P_f = \Delta P_t + \Delta P_{\rho p} = \Delta P_t + \rho_p E_p L \frac{g}{g_c} \tag{22}$$

The static head due to the gas, $\Delta P_{\rho g}$, is not included in Eq. 22 since the pressure lines of the manometer were filled with air in this experiment.

RESULTS AND DISCUSSION

Pressure Drop for Air Alone

The single-phase Fanning friction factors calculated from pressure drop data taken at various gas Reynolds numbers for air alone are shown in Figure 2 in comparison with the Nikuradse equation for a smooth tube. The experimental results agree within ±3% with the predicted values for turbulent flow. Scatter of data in the laminar flow region occurs mainly because the pressure difference between the measuring taps was too small to be accurately read on the manometer. The close agreement between measured and predicted values indicates that the flow section and instruments were reliable.

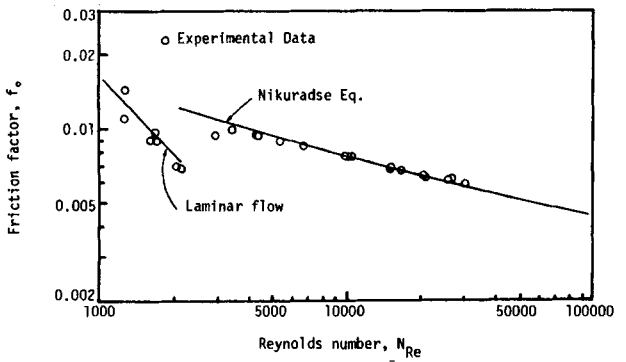

Figure 2. Friction factor with air alone.

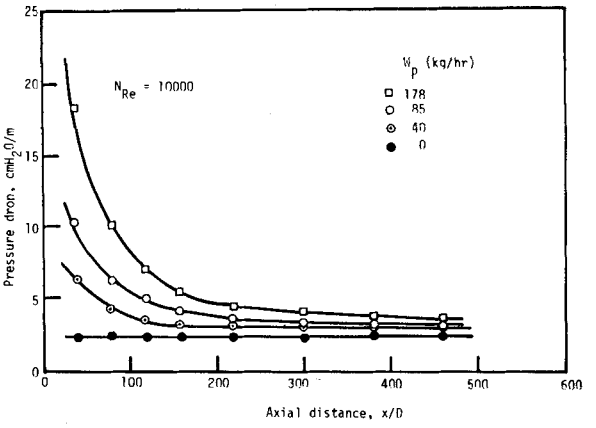

Figure 3. Effect of solids flow rate on hydraulic entry length, N_{Re} = 10,000.

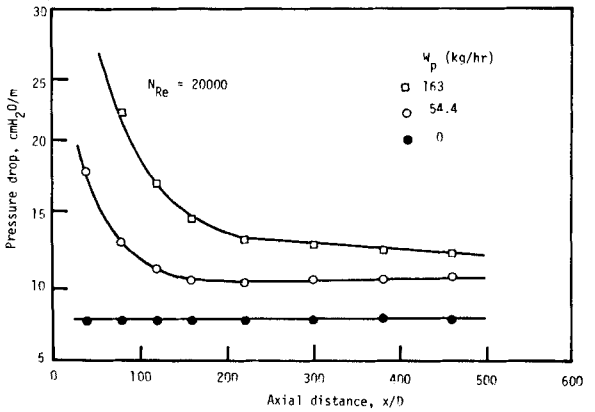

Figure 4. Effect of solids flow rate on hydraulic entry length, N_{Re} = 20,000.

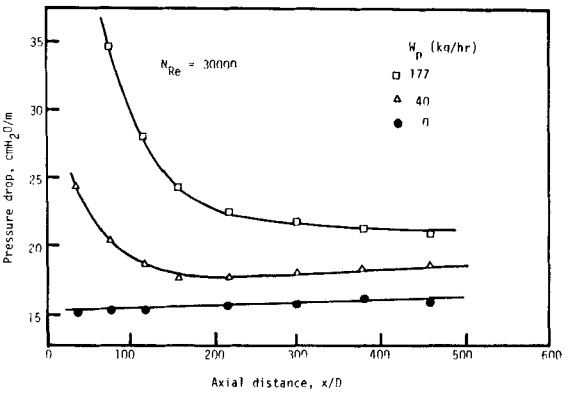

Figure 5. Effect of solids flow rate on hydraulic entry length, N_{Re} = 30,000.

Pressure Drop for Suspension Flow

For suspension flow, large pressure gradients are required to accelerate the particles in the upstream section where particles are introduced, and hence a longer hydraulic entry length is necessary than for flow of gas alone. Figures 3, 4, and 5 show the axial pressure-drop profiles at various solids flow rates for gas Reynolds numbers of 10,000, 20,000, and 30,000, respectively. The shaded circles in the figures represent the pressure drop for air alone, the friction factors of which were shown to agree with the correlation for single-phase flow. The hydraulic entry length is seen to be considerably prolonged by the addition of particles to the gas stream and is more dependent on the solids flow rate than it is on the gas Reynolds number. At a solids flow rate of 40 kg/h, the entry

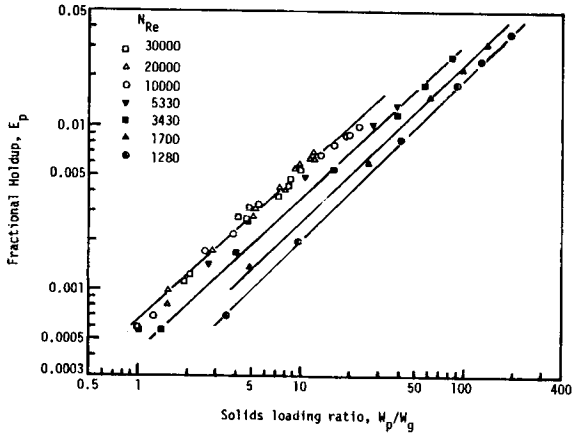

Figure 6. Correlation between solids loading ratio and holdup.

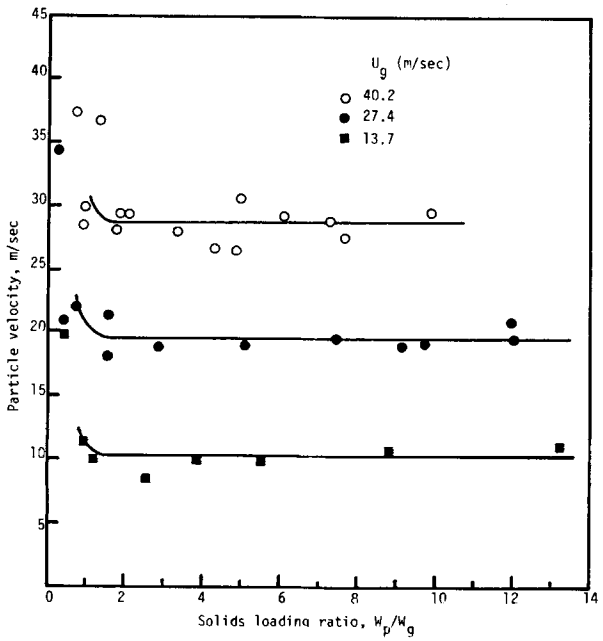

Figure 7. Effect of solids-loading ratio on particle velocity.

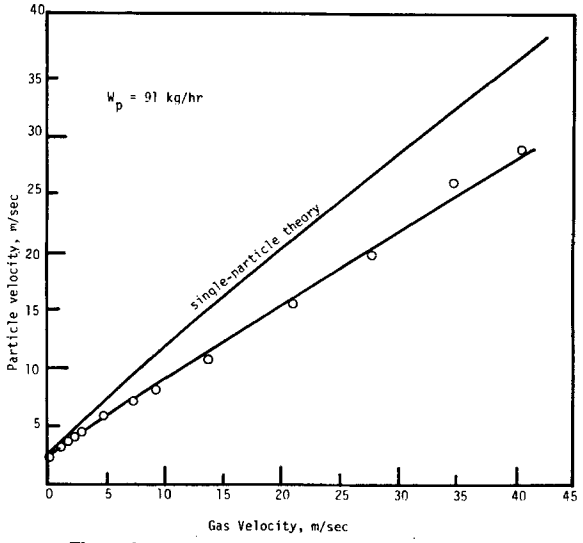

Figure 8. Effect of gas velocity on particle velocity.

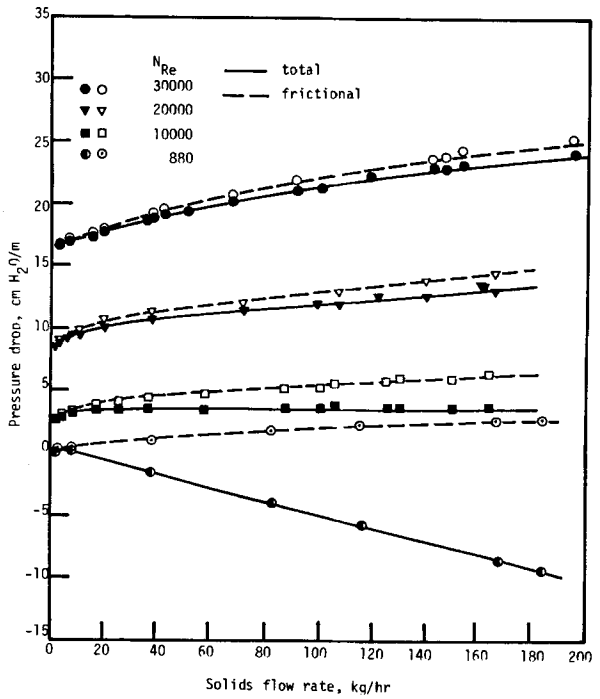

Figure 9. Effect of solids flow rate on total and frictional pressure drop.

length is about 120 diameters for gas Reynolds numbers of 10,000 and 30,000. Rose and Duckworth (1969) report similar observations that the length of pipe required for a particle to attain a steady velocity is independent of the gas Reynolds number for horizontal and upward transport of suspensions. Figures 3 to 5 also reveal that essentially fully developed flow conditions are achieved before reaching the holdup test section, which is located at an x/D ratio of 500.

Figure 6 shows the relationship between the particle holdup and the solids-loading ratio. For gas Reynolds numbers above 10,000, the particle holdup becomes independent of the gas Reynolds number, and all the data may be represented by the expression,

$$E_p = 0.00057 \frac{W_p}{W_g} \tag{23}$$

Particle velocities, as determined from the holdup data using Eq. 19 are plotted in Figure 7 as a function of solids-loading ratio for different gas Reynolds numbers, and in Figure 8 as a function of gas velocity at a fixed solids flow rate. Also included in Figure 8 is the particle velocity as calculated from the equation of motion of a single particle. From these figures, it is seen that, for gas velocities higher than 13.7 m/s, measured particle velocities are about 70% of the gas velocity; and experimental particle velocities are lower than the calculated values. A possible explanation for this lies in the effect of particle-wall friction, which gives additional resistance to the particles as they pass through the tube. For very dilute suspensions with loading ratios less than one, extremely small amounts of particles were trapped in the test section. The data taken in this region were not reliable since a significant portion was lost while collecting the particles. A sharp increase in particle velocity below a loading ratio of one, as seen in Figure 7, may be due to this error.

The effect of solids flow rate on the pressure drop for the fully developed region is shown in Figure 9. Both the total and frictional pressure drop are shown for four different gas Reynolds numbers. At low gas flow rates, e.g., a gas Reynolds number of 880, a negative total pressure drop can develop in the downflow system due to the negative sign of the hydrostatic head term in the pressure drop equation. However, the frictional pressure drop is always positive and is seen to be a weak function of the solids flow rate. At a gas Reynolds number of 10,000, the total pressure drop stays virtually constant for all solids flow rates covered after a slight increase at a very low solids flow rate. This indicates that the increased frictional pressure drop is balanced by the increase in the

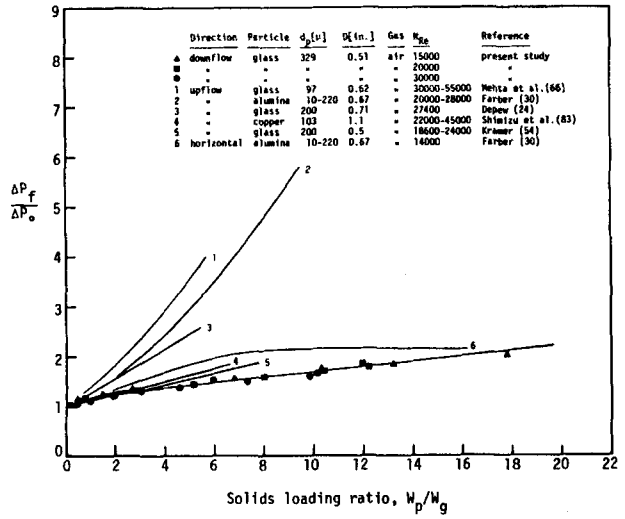

Figure 10. Comparison of specific pressure drop in downflow with upflow.

particle static head for all solids flow rates at this particular gas Reynolds number.

A comparison of the downflow data from this study with other data reported in the literature is shown in Figure 10, where specific pressure drop, defined as the ratio of the frictional pressure drop for the suspension to that for gas alone, is plotted against the solids-loading ratio. The data of Mehta et al. (1957) and Farber (1949) show very high specific pressure drop, which may have been due to the use of commercial pipes, with considerable surface roughness, for their test sections. The experimental conditions of Depew (1960) and Kramer (1970) are more similar to this research except that Kramer used glass tubing as a test section. No decisive conclusion can be made from this figure due to greatly different results of the upflow pressure drop even for comparable experimental conditions. Nevertheless, it is noticed that the specific pressure drop for downflow is a weaker function of the solids-loading ratio than for upflow, resulting in much lower pressure drops at high solids-loading ratios.

A plausible phenomenological explanation for the difference between upflow and downflow may be found by considering the motion of particles, especially those that enter near the wall region. In upflow, particles near the wall tend to flow downward due to gravity, and are picked up by the stream of particles flowing upward in the core region. The amount of recirculating particles is large at high solids-loading ratios or at low gas velocities, decreasing gradually as the solids-loading ratio is decreased or the gas velocity is increased. At higher gas velocities, where gravity-induced recirculation diminishes, additional particle recirculation induced by the Magnus force may become significant. It is well known that particles rotating in a shearing fluid experience a Magnus force, which is proportional to the rotational speed and the velocity gradient, and tend to move toward the region of higher velocity (Rubinow and Keller, 1961; Saffman, 1965). Indeed, Nakamura and Capes (1973), in their upflow experiments, report the existence of particle recirculation even at very high gas velocities.

The presence of recirculating particles incurs a relatively high friction loss since the lower velocity particles being picked up by the higher velocity stream generate additional turbulence in the flowing suspension. Compared to downflow, particles in the upflow system recirculate more due to the adverse gravity effect and Magnus force. In downflow, particle motion is assisted by gravity. Further, unlike upflow, particles in downflow do not experience velocity reversal, a fact implying less Magnus force on the particle. As a result, frictional loss in downflow is less than that in upflow as observed in Figure 10.

Correlation of the Frictional Pressure Drop

Applying the results of the similarity analysis, Figure 11 shows two-phase friction factors plotted against the gas Reynolds number,

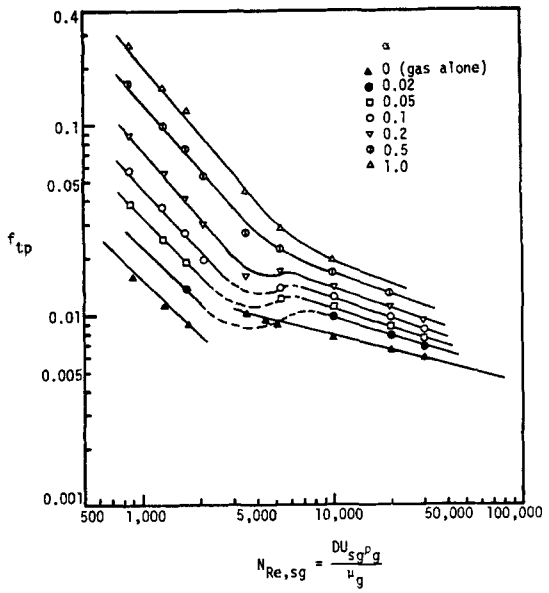

Figure 11. Correlation of two-phase friction factors.

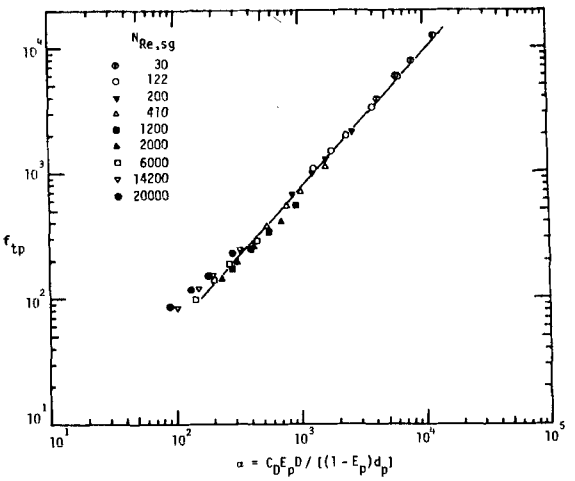

Figure 12. Correlation of pressure drop in packed beds.

$N_{Re,sg}$, based on the superficial gas velocity. The single-phase friction factor curve appears as a base line for a series of curves with various values of α. It appears that the apparent transition from laminar flow to turbulent flow is delayed, up to about 5,000, as the value of α increases; and at values above 0.5, the transition becomes smooth. This phenomenon suggests that adding more particles in a gas-solids two-phase flow, and hence increasing the value of α, may gradually stabilize the suspension flow, until the transition between laminar and turbulent flow becomes completely smooth. Similar observations have been reported for single-phase flows in curved tubes (Taylor, 1929) where secondary flow caused by centrifugal forces has a stabilizing effect that leads to a smoother transition from laminar to turbulent flow as the curvature ratio increases.

Generalization of the relation between the two-phase friction factor and α was attempted by applying the relationship indicated by Eq. 13 to a packed bed, which may be regarded as the upper limiting case of particle holdup. In Figure 12, pressure drop in a packed bed as given by Ergun's equation is recorrelated in terms of f_{tp} and α for the same range of variables as covered by Ergun. Figure 12 was prepared from Ergun's equation by taking the tube diameter as 1.3 cm to compare the absolute values of f_{tp} and α for a packed bed with those obtained in this study for dilute-phase flow. Although the points are somewhat scattered at low values of

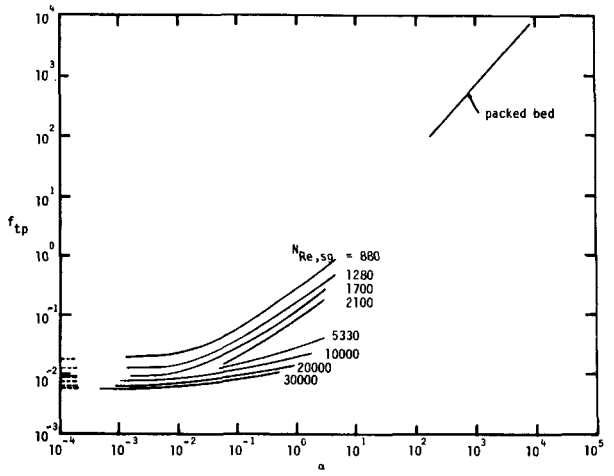

Figure 13. Generalized plot of friction factor curves.

α, it is seen that f_{tp} becomes independent of $N_{Re,sg}$ and can be represented by a straight line, as given by the equation

$$f_{tp} = 0.85\alpha \tag{23}$$

In Figure 13, the results for a downward dilute-phase flow and a packed-bed flow are shown together on a single plot. The parameter, α, as defined by Eq. 13, represents the ratio of the gas-particle interaction force to the gas-phase inertial force. This ratio is readily obtained from a steady-state form of the gas-phase momentum equation. Hence, from Eq. 8, we may approximate the inertial and gas-particle interaction forces by $(1 - E_p)\rho_g U_g^2/D$ and $3E_P C_D \rho_g U_g^2/4d_p$, respectively. The slip velocity is assumed to be a similar function of the gas velocity; for instance a linear relationship as measured in this study. The ratio therefore, yields the parameter α derived rigorously by a similarity analysis.

In view of the above physical meaning of α, it is of interest to consider its possibility as a universal correlating parameter covering the entire range from flow of gas alone to the packed bed. It is generally accepted that the gas-particle system involves several flow regimes with different physical phenomena. Previous investigators have analyzed distinct gas-solid systems on the basis of completely different approaches, examples being pressure drop correlations for the packed bed, moving bed, fluidized bed, dense- and dilute-phase conveying, and more recently the fast-fluidized bed. Considering the vast differences among these regimes, it may be presumptuous to suggest any parameter that can characterize all the flow regimes. Nevertheless, if attention is focused on the macroscopic manifestations of system flow characteristics, namely frictional pressure drop, it should be governed by frictional forces originating from the wall, represented by the gas Reynolds number, and the gas-particle interaction forces, accounted for by α.

Therefore, as shown in Figure 13, for a dilute-phase system, we see that wall friction and gas-particle interaction forces are both important. As gas-particle interaction forces diminish, curves for the dilute phase at the lower left corner reduce to those for gas alone.

For the other extreme case, i.e., a packed bed, it is seen that wall friction is negligible compared to the gas-particle interaction force, resulting in the disappearance of the Reynolds number as a separate parameter. Based on these results, it is proposed that the intermediate regions, i.e., moving bed, fluidized bed, etc., may also be correlated using the same parameter α. Unfortunately, for the intermediate dense-phase regimes, most investigators have not assessed the frictional pressure drop, largely because of the dominant static-head effect which is of more practical significance. From a fundamental point of view, the frictional component as defined here, is of more importance, and should be investigated. Although the flow regime boundaries, where the effect of $N_{Re,sg}$ becomes negligible, are not known at present, the effect of $N_{Re,sg}$ would gradually be diminished as dense-phase systems are entered.

The suggestion that the parameter α may have a universal applicability in the pressure drop correlation is undoubtedly speculative, and requires further investigation. However, the results here indicate that there is some evidence for a unified approach to correlating pressure drop for general gas-solids systems.

ACKNOWLEDGMENT

This work was supported by the United States Department of Energy under contract No. E(49-18)-2006. The interest and assistance of W. H. Wiser and R. E. Wood are greatly appreciated.

NOTATION

a = constant in Eq. 3
C_D = drag coefficient in a suspension
$C_{D,s}$ = drag coefficient of a single particle in an infinite medium
d_p = particle diameter
D = tube diameter
E_p = particle holdup
f_m = mixture friction factor, defined in Eq. 3
f_p = solids friction factor, defined in Eq. 2
f_{tp} = two-phase friction factor, defined in Eq. 12
g = acceleration due to gravity
g_c = Newton's law conversion factor
G_g = gas mass velocity
G_p = particle mass velocity
L = distance between the pressure taps
n = constant in Eq. 15
$N_{Re,sg}$ = Reynolds number based on the superficial velocity of the gas, $DU_{sg}\rho_g/\mu_g$
P = pressure
ΔP_{ag} = acceleration pressure drop due to gas
ΔP_{ap} = acceleration pressure drop due to particles
ΔP_f = friction pressure drop
ΔP_{fg} = friction pressure drop due to gas
ΔP_{pf} = excess pressure drop caused by addition of particles
ΔP_t = total pressure drop
$\Delta P_{\rho g}$ = static pressure drop due to gas
$\Delta P_{\rho p}$ = static pressure drop due to particles
r = radial distance
t = time
U_g = gas velocity
U_p = particle velocity
U_{sg} = superficial gas velocity
U_{sp} = superficial particle velocity
V_s = slip velocity
W_g = gas flow rate
W_p = particle flow rate
x = axial distance

Greek Letters

α = dimensionless parameters, $C_D E_p D/[1 - E_p)d_p]$
μ_g = gas viscosity
μ_{gm} = viscosity of gas phase in a suspension
μ_{pm} = viscosity of particle phase in a suspension
ρ_{dg} = dispersed gas density
ρ_{dp} = dispersed particle density
ρ_g = gas density
ρ_p = particle density
ψ_1, ψ_2 = denote functions of, in Eqs. 11 and 13

LITERATURE CITED

Boothroyd, R. G., *Flowing Gas-Solids Suspensions*, Chapmann and Hall, Ltd, 11 New Fetter Lane, London (1971).

Capes, C. E., and K. Nakamura, "Vertical Pneumatic Conveying: An Experimental Study with Particles in the Intermediate and Turbulent Flow Regimes," *Can. J. Chem. Eng.*, **51**, 31 (1973).
Churchill, S. W., *The Interpretation and Use of Rate Data: The Rate Concept*, McGraw-Hill, New York (1974).
Depew, C. A., "Heat Transfer to Flowing Gas-Solids Mixtures in a Vertical Duct," Ph.D. Thesis, University of California, Berkeley (1960).
Doig, I. D., and G. H. Roper, "Air Velocity Profiles in the Presence of Cocurrently Transported Particles," *Ind. Eng. Chem. Fund.*, **6**, 247 (1967).
Ergun, S., "Fluid Flow Through Packed Columns," *Chem. Eng. Prog.*, **48**, 89 (1952).
Farber, L., "Flow Characteristics of Solids-Gas Mixture in a Horizontal and Vertical Circular Conduit," *Ind. Eng. Chem.*, **41**, 1184 (1949).
Friedlander, S. K., "Behavior of Suspended Particles in a Turbulent Fluid," *AIChE J.*, **3**, 381 (1957).
Gasterstaedt, J., "Die Experimentelle Undersuchung des Pneumatischen Fordervorganges," *Zeit. Vereines Deutscher Ingenieure*, **68**, 617 (1924).
Gel'perin, N. I., V. G. Aynshteyn, L. I. Krupnik, and Z. N. Memedlyayer, "Pressure Losses in Gas-Conveyed Solid Suspension Flows," *Fluid Mechanics-Soviet Research*, **5**, No. 4, 4 (1976).
Gill, W. N., and M. Scher, "A Modification of the Momentum Transport Hypothesis," *AIChE J.*, **7**, 61 (1961).
Hariu, O. H., and M. C. Molstad, "Pressure Drop in Vertical Tubes in Transport of Solids by Gases," *Ind. Eng. Chem.*, **41**, 1148 (1949).
Hellums, J. D., and S. W. Churchill, "Dimensional Analysis and Natural Circulation," *Chem. Eng. Prog. Symp. Ser.*, **57**, No. 32, 75 (1961).
Hinze, J. O., "Momentum and Mechanical-Energy Balance Equations for a Flowing Homogeneous Suspension with Slip between the Two Phases," *Appl. Sci. Res.*, Section A, **11**, 33 (1962).
Jones, J. H., W. E. Braun, T. E. Daubert, and H. D. Allendorf, "Estimation of Pressure Drop for Vertical Pneumatic Transport of Solids," *AIChE J.*, **13**, 608 (1967).
Julian, F. M., and A. E. Dukler, "An Eddy Viscosity Model for Friction in Gas-Solids Flow," *AIChE J.*, **11**, 853 (1965).
Khan, J. I., and D. C. Pei, "Pressure Drop in Vertical Solid-Gas Suspension Flow," *Ind. Eng. Chem. Process Des. Dev.*, **12**, 428 (1973).
Kim, J. M., "Pressure Drop and Heat Transfer in Cocurrent Downflow of Gas-Solids Suspensions," Ph.D. Thesis, University of Utah, Salt Lake City, UT (1979).
Konno, H., and S. Saito, "Pneumatic Conveying of Solids Through Straight Pipes," *J. of Chem. Eng. of Japan*, **2**, 211 (1969).
Kramer, T. J., "Mean Flow Characteristics of Flowing Gas-Solids Suspensions," Ph.D. Thesis, University of Washington, Seattle, WA (1970).
——, and C. A. Depew, "Analysis of Mean Flow Characteristics of Flowing Gas-Solids Suspensions," *Trans. of ASME, J. Basic Eng.*, **94D**, 731 (1972).
Ladelfa, C. J., and M. I. Greene, "Economic Evaluation of Synthetic Natural Gas Production by Short Residence Time Hydropyrolysis of Coal," *Fuel Proc. Tech.*, **1**, 187 (1977/1978).
Leung, L. S., and R. J. Wiles, "A Quantitative Design Procedure for Vertical Pneumatic Conveying Systems," *Ind. Chem. Process Des. Dev.*, **15**, 552 (1976).
Mehta, N. C., J. M. Smith, and E. W. Comings, "Pressure Drop in Air-Solid Flow Systems," *Ind. Eng. Chem.*, **49**, 986 (1957).
Nakamura, K., and C. E. Capes, "Vertical Pneumatic Conveying: A Theoretical Study of Uniform and Annular Particle Flow Models," *Can. J. Chem. Eng.*, **51**, 39 (1973).
Peskin, R. L., "Some Effects of Particle-Particle and Particle-Fluid Interactions in Two-Phase Flow Systems," Ph.D. Thesis, Princeton (1959).
Reddy, K. V. S., and D. C. T. Pei, "Particle Dynamics in Solids-Gas Flow in a Vertical Pipe," *Ind. Eng. Chem. Fund.*, **8**, 490 (1969).
Richardson, J. F., and M. McLeman, "Pneumatic Conveying—Part II Solids Velocities and Pressure Gradients in a One-inch Horizontal Pipe," *Trans. Instn. Chem. Engrs.*, **38**, 257 (1960).
Rose, H. E., and H. E. Banacle, "Flow of Suspensions of Non-cohesive Spherical Particles in Pipes," *The Engineer*, **203**, 898 (1957).
Rose, H. E., and R. A. Duckworth, "Transport of Solid Particles in Liquids and Gases," *The Engineer*, **227**, 392, 430 (1969).
Rubinow, S. I., and J. B. Keller, "The Transverse Force on a Spinning Sphere Moving in a Viscous Fluid," *J. Fluid Mech.*, **11**, 447 (1961).
Saffman, P. G., "The Lift on a Sphere in a Slow Shear Flow," *J. Fluid Mech.*, **22**, 385 (1965).
Shimizu, A., R. Echigo, S. Hasegawa, and M. Hishida, "Experimental Study on the Pressure Drop and the Entry Length of the Gas-Solids Suspension Flow in a Circular Tube," *Int. J. Multiphase Flow*, **4**, 53 (1978).
Soo, S. L., *Fluid Dynamics of Multiphase Systems*, Ginn & Blaisdell Publishing Co., Waltham, MA (1967).
Soo, S. L., "Fully Developed Turbulent Pipe Flow of a Gas-Solids Suspension," *Ind. Eng. Chem. Fund.*, **1**, 33 (1962).
Soo, S. L., and J. A. Regalbuto, "Concentration Distribution in Two-Phase Pipe Flow," *Can. J. Chem. Eng.*, **38**, 160 (1960).
Taylor, G. I., "The Criterion for Turbulence in Curved Pipes," *Proc. Roy. Soc. London*, **A124**, 243 (1929).
Van Deemter, J. J., and E. T. Van der Laan, "Momentum and Energy Balances for Dispersed Two-Phase Flow," *Appl. Sci. Res.*, **10**, 103 (1961).
Vogt, E. G., and R. R. White, "Friction in the Flow of Suspensions: Granular Solids in Gases through Pipe," *Ind. Eng. Chem.*, **40**, 1731 (1948).
Wen, C. Y., and Y. H. Yu, "Mechanics of Fluidization," *Chem. Eng. Prog., Symp.*, **62**, 100 (1966).
Wood, R. E., and W. H. Wiser, "Coal Liquefaction in Coiled Tube Reactors," *Ind. Eng. Chem. Process Des. Dev.*, **15**, 144 (1976).
Yang, Wen-Ching, "Correlations for Solid Friction Factors in Vertical and Horizontal Pneumatic Conveyings," *AIChE J.*, **24**, 548 (1978).

Manuscript received June 4, 1981; revision received May 18, and accepted June 18, 1982.